

Synthesis of a Uranium(VI)-Carbene: Reductive Formation of Uranyl(V)-Methanides, Oxidative Preparation of a $[R_2C=U=O]^{2+}$ Analogue of the $[O=U=O]^{2+}$ Uranyl Ion ($R = Ph_2PNSiMe_3$), and Comparison of the Nature of $U^{IV}=C$, $U^V=C$, and $U^{VI}=C$ Double Bonds

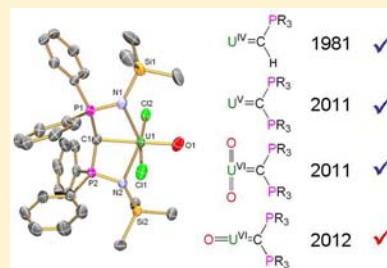
David P. Mills,[†] Oliver J. Cooper,[†] Floriana Tuna,[‡] Eric J. L. McInnes,[‡] E. Stephen Davies,[†] Jonathan McMaster,[†] Fabrizio Moro,[†] William Lewis,[†] Alexander J. Blake,[†] and Stephen T. Liddle^{*,†}

[†]School of Chemistry, University of Nottingham, University Park, Nottingham NG7 2RD, U.K.

[‡]EPSRC National UK EPR Facility, School of Chemistry and Photon Science Institute, The University of Manchester, Oxford Road, Manchester M13 9PL, U.K.

Supporting Information

ABSTRACT: We report attempts to prepare uranyl(VI)- and uranium(VI) carbenes utilizing deprotonation and oxidation strategies. Treatment of the uranyl(VI)-methanide complex $[(BIPMH)UO_2Cl(THF)]$ [1, BIPMH = $HC(PPh_2NSiMe_3)_2$] with benzylsodium did not afford a uranyl(VI)-carbene via deprotonation. Instead, one-electron reduction and isolation of di- and trinuclear $[UO_2(BIPMH)(\mu-Cl)UO(\mu-O)\{BIPMH\}]$ (2) and $[UO(\mu-O)(BIPMH)(\mu_3-Cl)\{UO(\mu-O)(BIPMH)\}_2]$ (3), respectively, with concomitant elimination of dibenzyl, was observed. Complexes 2 and 3 represent the first examples of organometallic uranyl(V), and 3 is notable for exhibiting rare cation–cation interactions between uranyl(VI) and uranyl(V) groups. In contrast, two-electron oxidation of the uranium(IV)-carbene $[(BIPM)UCl_3Li(THF)_2]$ (4) by 4-morpholine *N*-oxide afforded the first uranium(VI)-carbene $[(BIPM)UOCl_2]$ (6). Complex 6 exhibits a *trans*-CUO linkage that represents a $[R_2C=U=O]^{2+}$ analogue of the uranyl ion. Notably, treatment of 4 with other oxidants such as Me_3NO , C_5H_5NO , and TEMPO afforded 1 as the only isolable product. Computational studies of 4, the uranium(V)-carbene $[(BIPM)UCl_2I]$ (5), and 6 reveal polarized covalent $U=C$ double bonds in each case whose nature is significantly affected by the oxidation state of uranium. Natural Bond Order analyses indicate that upon oxidation from uranium(IV) to (V) to (VI) the uranium contribution to the $U=C$ σ -bond can increase from ca. 18 to 32% and within this component the orbital composition is dominated by 5f character. For the corresponding $U=C$ π -components, the uranium contribution increases from ca. 18 to 26% but then decreases to ca. 24% and is again dominated by 5f contributions. The calculations suggest that as a function of increasing oxidation state of uranium the radial contraction of the valence 5f and 6d orbitals of uranium may outweigh the increased polarizing power of uranium in 6 compared to 5.



INTRODUCTION

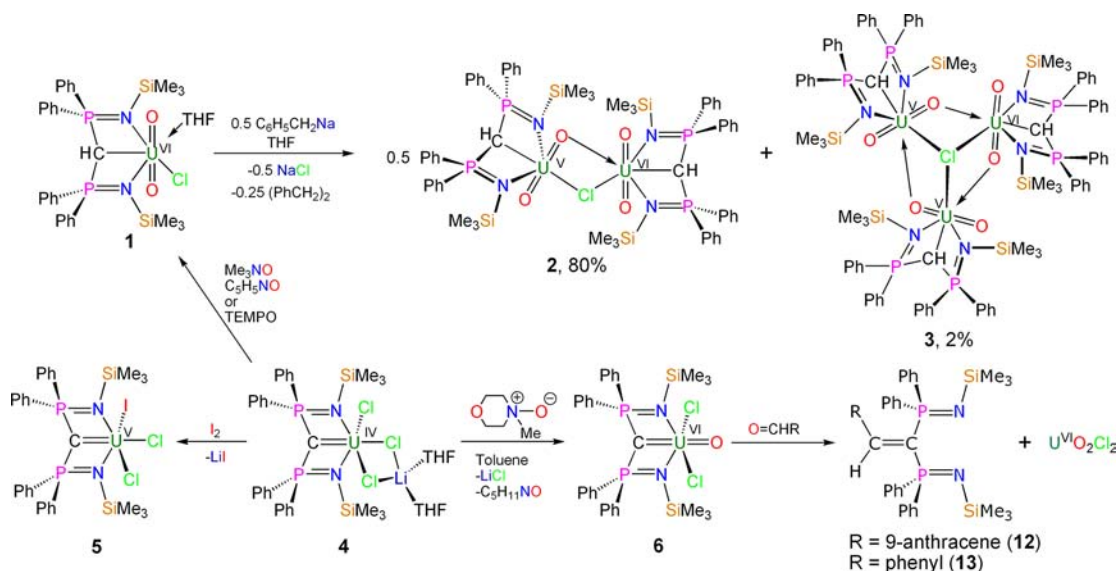
Carbene complexes of the transition metals are well established due to their prominent synthetic applications,¹ and they are known over a range of low (Fischer carbenes) to high (Schrock alkylidenes) formal oxidation states.² However, the corresponding f-block metal–carbon multiple bond chemistry is underdeveloped.³ The first uranium–carbene, $[(\eta^5-C_5H_5)_3U=C(H)PMe_2Ph]$, was reported in 1981,⁴ but nearly three decades passed⁵ before the area developed further,⁶ and, in contrast to d-block carbenes, all uranium–carbenes were limited to uranium(IV).^{4,6} However, very recently, the first uranyl(VI)-⁷ and uranium(V)-carbenes⁸ have been reported giving insight into the nature of uranium–carbon multiple bonding. Conspicuous by its absence is any report of a uranium(VI)-carbene.⁹ Given the paucity of high oxidation state uranium–carbenes, we attempted to access uranyl(VI)- and uranium(VI)-carbenes.

Recent work by some of us^{6c,f,8} has exploited the bis(iminophosphorano)methanediide pincer-carbene ligand BIPM $[BIPM = C(PPh_2NSiMe_3)_2]$ in the coordination sphere of uranium since the chelating iminophosphorano arms stabilize any uranium–carbene interactions. In order to access high-valent uranium–carbenes we identified deprotonation of a uranyl-methanide precursor, or oxidation of a uranium(IV) carbene, as attractive and complementary synthetic approaches.

Although attempts to prepare organometallic derivatives of UO_2^{2+} date back to the 19th century,¹⁰ such complexes are rare.^{7,11,12} It is germane to note that analogous rare earth methanides can be converted to carbenes by treatment with alkali metal bases.¹³ Thus, in principle, deprotonation of a methanide uranyl halide complex could effect formation of a

Received: February 9, 2012

Published: May 23, 2012

Scheme 1. Synthesis of 2, 3, 5, 6, 12, and 13^a

^aAll terminal oxo groups form formal triple bonds to uranium through two polarized covalent and one dative contribution from oxygen to uranium, but for clarity the dative donation is omitted. The syntheses of 1, 4, and 5 are described in refs 11b and 8.

uranyl carbene with concomitant salt elimination. However, a competing reaction path for uranyl(VI) is reduction to uranyl(V) with concomitant elimination of oxidatively coupled alkyl. Nevertheless, the isolation of organometallic uranyl(V) complexes would in itself be significant because, to date, only ligands containing nitrogen and oxygen donor centers, such as pyridines, phosphine oxides, salens, diketonate/-iminate derivatives, and macrocycles have stabilized UO_2^{+} .¹⁴ Aside from fundamental interest, the chemistry of actinyl cations, $\text{AnO}_2^{+/2+}$, plays a central role in nuclear technology and environmental actinide mobility.¹⁵ Cation–cation interactions (CCIs),¹⁶ where a uranyl oxo atom acts as a Lewis base to another uranyl uranium center, play a crucial role in the solid-state and solution chemistry of the actinyls, and while the oxo groups in uranyl(VI), UO_2^{2+} , are rarely involved in the coordination to other cations,^{17,18} CCIs have been increasingly observed in UO_2^{+} derivatives. The reactivity of CCIs has important environmental implications because UO_2^{+} species have been identified as key intermediates in anaerobic bacterial- and mineral-mediated reduction of soluble UO_2^{2+} to insoluble uranium(IV) compounds.¹⁹

Previous work has established that uranium(IV)-carbenes utilizing the BIPM framework can undergo one-electron oxidation with the weak oxidant iodine.⁸ However, no further tractable oxidation of uranium could be accomplished without apparent oxidation of the BIPM ligand. We therefore concluded that a concerted two-electron oxidation utilizing *N*-oxides represented the most feasible approach to a uranium(VI)-carbene.^{14a} Herein, we report that our work has resulted in one-electron reduction of uranyl(VI)-methanides to give organometallic uranyl(V) complexes; conversely, two-electron oxidation of a uranium(IV)-carbene has afforded a uranium(VI)-carbene, which exhibits a *trans*-CUO linkage that represents a $[\text{R}_2\text{C}=\text{U}=\text{O}]^{2+}$ analogue of the uranyl ion.²⁰

RESULTS AND DISCUSSION

Attempted Deprotonation of a Uranyl(VI) Methanide.

Our initial efforts targeted $[(\text{BIPMH})\text{UO}_2\text{Cl}(\text{THF})]$ [1,

$\text{BIPMH} = \text{HC}(\text{PPh}_2\text{NSiMe}_3)_2$].^{11b} We treated 1 with benzylsodium (Scheme 1) and found, unlike the rare earth congeners, that elimination of NaCl was accompanied by elimination of dibenzyl and reduction of uranyl(VI) to uranyl(V) rather than effecting methanide deprotonation. The slow elimination of chloride from 1 in this reaction apparently results in the uranyl(V) fragment being trapped by unreacted 1 to afford the organometallic CCI complex $[\text{UO}_2(\text{BIPMH})(\mu\text{-Cl})\text{UO}(\mu\text{-O})(\text{BIPMH})]$ (2) in 80% yield as yellow crystals, but intermediates could not be observed. Complex 2 is formed irrespective of the ratio of benzyl sodium to 1 and attempts to react 1 with other alkali metal alkyls, amides, and hydrides, e.g. $[\text{C}_5\text{Me}_5\text{K}]$,²¹ gave intractable reaction mixtures.

The $^{31}\text{P}\{^1\text{H}\}$ NMR spectrum of 2 exhibits sharp (−5.16 ppm) and broad (−129.42 ppm) resonances attributed to the diamagnetic UO_2^{2+} (cf. 8.00 ppm for 1^{11b}) and paramagnetic UO_2^{+} BIPMH ligands, respectively. The ^1H NMR spectrum exhibits sharp diamagnetic and broad paramagnetically shifted resonances; the methanide protons resonate at 3.40 ($^2J_{\text{PH}} = 14$ Hz; cf. 2.28 ppm, $^2J_{\text{PH}} = 11$ Hz for 1) and −4.14 ppm (broad singlet) and two silyl resonances at 0.38 (sharp) and −9.68 (broad) ppm were observed. The magnetic moment of 2 in benzene at 298 K is $2.59 \mu_{\text{B}}$ and this is consistent with the presence of one $^2\text{F}_{5/2}$ UO_2^{+} center (theoretical $\mu_{\text{eff}} = 2.54 \mu_{\text{B}}$).²² This paramagnetism is confirmed by the observation of EPR spectra (S- and K-band²³) of solid-state samples below 20 K. The spectra are rhombic with an effective $S = 1/2$ with the two larger g_{eff} components being 3.8 and 3.7; these both appear as doublets and although this fine structure can be simulated as hyperfine coupling ($I = 1/2$, $a_1 = 120 \times 10^{-4}$, $a_2 = 100 \times 10^{-4} \text{ cm}^{-1}$ and arbitrarily small a_3 ; in the effective spin doublet approximation) its origin at this stage is not clear. The FTIR spectrum of 2 exhibits stretches at 906, 835, and 803 cm^{-1} , which we attribute to the UO_2^{2+} and UO_2^{+} groups, respectively. These values compare to values of 908, 853, 797, and 800 cm^{-1} for 1,^{11b} $\text{UO}_2(\text{OTf})(\text{THF})_n$, $[\text{UO}_2(\text{Py})_5]^+$, and $[\text{UO}_2\{\text{HC}(\text{CMe}_2\text{NDipp})_2\}(\text{OPMePh}_2)_2]$ (Dipp = 2,6- $\text{Pr}_2\text{C}_6\text{H}_3$).²⁴

The molecular structure of 2, which confirms the CCI formulation, is illustrated in Figure 1. Each uranyl center is

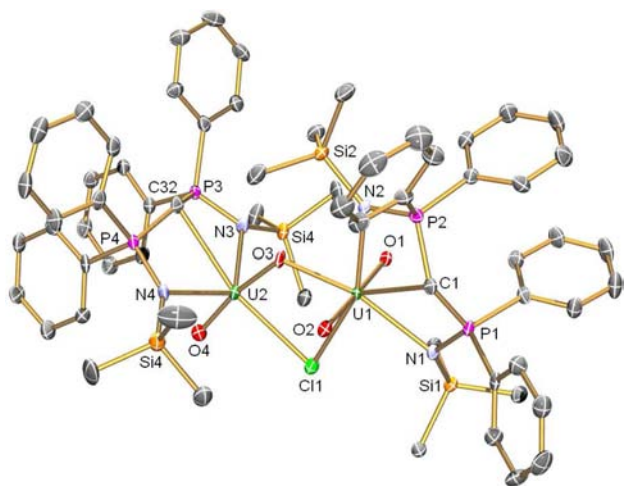


Figure 1. Molecular structure of **2** with selective labeling and displacement ellipsoids set at 40%; hydrogen atoms and toluene lattice solvent omitted for clarity.

ligated by a BIPMH ligand and the dinuclear structure is generated by a bridging chloride [U1–Cl1 2.8560(15); U2–Cl1 2.8089(14) Å] and a bridging O3 oxo group from U2 to U1. The U1–O1 and U1–O2 bond lengths of 1.785(4) and 1.776(4) Å, respectively, are within the range for uranyl(VI) U–O bond distances;²⁵ this compares to U2–O3 and U2–O4 bond lengths of 1.932(4) and 1.843(5) Å, respectively, which are considerably longer, but in line with previously reported covalent bridging and terminal uranyl(V) U–O bond distances.¹⁷ The U2–O3 bond length is particularly long, reflecting the U1–O3 dative bridge of 2.316(4) Å. The U1–C1 bond length of 2.732(6) Å is longer than in **1** [2.681(1) Å],^{11b} which reflects the more sterically congested environment in **2** compared to **1**. The U2–C32 bond distance of 2.735(6) Å is invariant to the U1–C1 distance, however there are no other uranyl(V)-carbon bond distances with which to compare. Overall, the metrical data suggest that U(1) and U(2) can be assigned as UO_2^{2+} and UO_2^+ centers, respectively, in agreement with the magnetic data.

From the reaction which yielded **2** we also isolated a small number (2% yield) of red blocks by fractional crystallization identified as $[\text{UO}(\mu\text{-O})(\text{BIPMH})(\mu_3\text{-Cl})\{\text{UO}(\mu\text{-O})(\text{BIPMH})\}_2]$ (**3**) (Scheme 1). In contrast to **2**, the $^{31}\text{P}\{\text{H}\}$ NMR spectrum of **3** exhibits a sharp singlet at -5.17 ppm and a poorly resolved, paramagnetically broadened AB-type quartet centered at -149.44 ppm ($^2J_{\text{PP}}$ not resolved due to line broadening) suggestive of inequivalent P-centers in BIPMH ligands bound to UO_2^+ . The ^1H NMR spectrum of **3** is complex, indicating asymmetric ligand environments in solution. The methanide protons resonate at 3.28 ($^2J_{\text{PH}} = 14$ Hz) and -4.27 (paramagnetically broadened singlet) ppm and three silyl environments in the ratio 18:18:18H are observable as well as numerous phenyl proton environments. The magnetic moment of **3** in benzene at 298 K is $4.01 \mu_{\text{B}}$, which is consistent with the presence of two UO_2^+ centers and compares to a theoretical moment of $3.60 \mu_{\text{B}}$ for two isolated UO_2^+ centers. The FTIR spectrum of **3** exhibits a complex and overlapping band structure in the region $910\text{--}802 \text{ cm}^{-1}$ but the strongest identifiable stretch at 802 cm^{-1} compares well to **2** and can be assigned as a UO_2^+ stretch.

The structure of **3** (Figure 2) was determined and found to adopt a trinuclear CCI structure which is constructed through

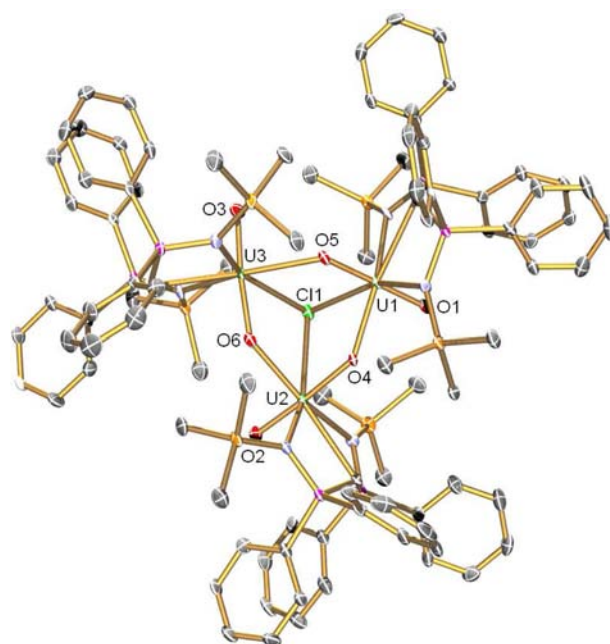


Figure 2. Molecular structure of **3** with selective labeling and displacement ellipsoids set at 40%; hydrogen atoms and toluene lattice solvent omitted for clarity.

three bridging uranyl oxo groups and a μ_3 -chloride. This results in an open cubane with one vacant vertex. The coordination sphere of each uranyl center is completed by a BIPMH ligand. The three terminal U1–O1, U2–O2, and U3–O3 distances and three bridging oxo U1–O5, U2–O4, and U3–O6 distances of 1.776(4), 1.825(4), and 1.8822(4) Å, and 1.812(4), 1.966(4), and 1.903(4) Å, respectively, suggest that the U1, U2, and U3 oxidation states can be unambiguously assigned as VI, V, and V, respectively, in agreement with the magnetic data. The dative U1–O4, U2–O6, and U3–O5 bond lengths are 2.239(4), 2.360(4), and 2.544(4) Å, respectively. The first two dative bond length values are comparable to **2**, and the short U1–O4 distance reflects the fact that U1 is hexavalent, but the latter value is long. We suggest this is a result of the lower Lewis basicity of this oxo group, which derives from a hexavalent uranyl group, compared to the more Lewis basic UO_2^+ oxo groups. The U2–Cl1 and U3–Cl1 bond lengths of 2.969(2) and 2.956(2) Å are both ~ 0.1 Å longer than the U1–Cl1 bond length of 2.858(2) Å, which reflects their UO_2^+ and UO_2^{2+} formulations, respectively. The U1–C1, U2–C32, and U3–C63 bond lengths of 2.652(5), 2.709(6), and 2.717(5) Å, respectively, are shorter than observed in **2**, which may derive from μ_3 -Cl-bridged **3** exhibiting more electron-deficient uranyl centers than in μ_2 -Cl-bridged **2**, and is in-line with the assigned uranyl oxidation states.

Discussion of the Reduction Chemistry of a Uranyl(VI) Methanide. In contrast to rare earth BIPMH methanides which can be converted to the corresponding carbenes by deprotonation,¹³ it would seem that for uranyl(VI) reduction by nucleophilic alkyls represents a more favorable reaction pathway. Germane to this point, reduction of bis(imido) uranyl(VI) analogues by alkyls has also been noted.²¹ Thus, a uranyl(VI)-carbene would appear to be inaccessible via a deprotonation pathway for BIPMH complexes. This contrasts to uranyl(VI) complexes stabilized by the $\text{C}(\text{PPh}_2\text{S})^{2-}$ dianion where deprotonation methods were found to be viable.⁷

Complexes **2** and **3** are significant because they represent the first examples of organometallic uranyl(V) complexes since all other examples of uranyl(V) are stabilized by ligands containing nitrogen or oxygen donor centers, such as pyridines, phosphine oxides, salens, diketonate/-imate derivatives, and macrocycles.¹⁴ Typically, uranyl(VI) oxos are poor Lewis base donors because of the strong uranium–oxygen triple bonds. However, $5f^1$ uranyl(V) presents electronic repulsion and thus the oxo centers become more Lewis basic. Thus, the involvement of uranyl(VI)-uranyl(V) CCI in **3** is noteworthy. The nature of such CCI is important to understand given the environmental implications for AnO_2^{+2+} mobility. Unfortunately, solutions of **2** and **3** in toluene decompose on standing to afford a complex mix of unidentified products. This has precluded detailed solution studies, but **2** and especially **3** highlight the complex nature of CCI chemistry.

Two-Electron Oxidation of a Uranium(IV)-Carbene To Give a Uranium(VI)-Carbene. Realizing that reduction of uranyl(VI) to uranyl(V)-containing products is facile for **1**, we turned from a deprotonation method to an oxidation strategy utilizing $[(BIPM)UCl_3Li(THF)_2]$ (**4**), as this complex is the precursor to the uranium(V)-carbene $[(BIPM)UCl_2I]$ (**5**).⁸ Treatment of **4** with 1 equiv of 4-morpholine *N*-oxide gave $[(BIPM)UOCl_2]$ (**6**) after workup in 52% crystalline yield as brown blocks (Scheme 1). The NMR spectra of **6** are diamagnetic, and the characterization data support the formulation. The FTIR spectrum of **6** exhibits a stretch at 917 cm^{-1} which is attributed to the uranium-oxo group.

The molecular structure of **6** is illustrated in Figure 3. We experienced considerable difficulty obtaining any crystals of **6**

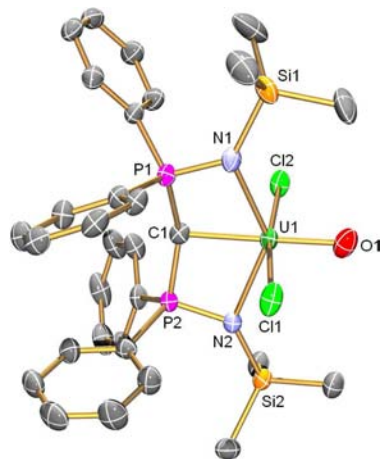


Figure 3. Molecular structure of **6** with selective labeling and displacement ellipsoids set at 40%; hydrogen atoms, toluene lattice solvent, and disorder components omitted for clarity.

suitable for X-ray crystallography. The majority of our attempts resulted in microcrystalline materials of pure **6**. However, one crystallization attempt yielded a crystal of sufficient quality for diffraction studies but the resulting structure was found to exhibit disorder. In this crystal, complex **6** is present in 75% occupancy; the remaining 25% being occupied by $[(BIPM)UCl_3]$ (which we label as **5a** in order to differentiate it from the iodo-dichloro analogue **5**) with both components centering on the same uranium position. The relative occupancies were determined by competitive refinement. Because of the low occupancy of this pentavalent impurity the 25% “shadow” BIPM ligand component could not be located²⁶ but the heavy chloride was located and successfully modeled. The geometric and thermal parameters are reasonable and consistent with literature values so the minor component is not affecting the major one and we are therefore confident that the structural refinement represents **6**. Despite this disorder, the bulk purity of **6** was established from the spectroscopic and analytical data. We analyzed the crystal used for the data collection by 1H NMR spectroscopy and observed a mixture of **6** and **5a** in a 72:25 ratio which corroborates the disorder.²³ The disorder most likely arises from partial oxidation of **4**. The most salient point of **6** is that the oxo group resides *trans* to the carbene $[C1-U1-O1 \angle = 175.54(15)^\circ]$, which we ascribe to the inverse *trans* influence (ITI).²⁷ The $U1-C1$ bond distance of $2.184(3)\text{ \AA}$ is the shortest $U-C$ distance on record,²⁵ reflecting the hexavalent state of **6**, and it compares to $U=C$ bond distances of $2.310(4)$, $2.268(10)$, and $2.29(3)\text{ \AA}$ observed in closely related $U(IV)$ **4**,⁸ $U(V)$ **5**,⁸ and $U(IV)$ $[(\eta^5-C_5H_5)_3U=C(H)PMe_2Ph]$,^{4a} respectively. The $U-N$ bond distances (av. 2.313 \AA) in **6** are substantially shorter than in **4** but longer than in **5**. Conversely, the $U-Cl$ bonds in **6** (av. 2.623 \AA) are not significantly different to **4** but are shorter than in **5**. The $U1-O1$ distance of $1.841(4)\text{ \AA}$ in **6** is within the range of hexavalent uranyl $U-O$ bond distances.²⁵ Complex **6** exhibits a *trans*-CUO linkage, which is a $[R_2C=U=O]^{2+}$ analogue of the uranyl ion previously observed only in matrix isolation experiments.²⁰ The $[R_2C=U=O]^{2+}$ linkage adds to the $[E=U=O]^{2+}$ ($E=O, N, C$) family^{12,20,28} which is of general interest due to potential E and O atom transfer chemistry.

In contrast to the reaction outcome observed when 4-morpholine *N*-oxide is employed, when **4** was treated with one equivalent of *N*-oxides such as Me_3NO , C_5H_5NO , and TEMPO only complex **1**,^{11b} could be isolated (Scheme 1). To account for these observations we suggest that Me_3NO , C_5H_5NO , and TEMPO may bind to **4**, and exhibit $N-O$ cleavage, with greater rates than 4-morpholine *N*-oxide, thus resulting in overoxidation. In contrast, 4-morpholine *N*-oxide may bind more slowly with a moderate $N-O$ cleavage rate enabling mild oxidation. This is in part supported by the observation of **5a**

Table 1. Selected Experimental and Computed Data for Tetravalent **4**, Pentavalent **5**, and Hexavalent **6**

entry ^a	bond lengths and indices			atomic spin-densities and charges			$U=C$ σ -component ^h			$U=C$ π -component ^h			ref
	$U-C^b$	$U-C^c$	BI^d	m_U^e	q_U^f	q_C^g	C%	U%	U 6d:5f	C%	U%	U 6d:5f	
4	2.310(4)	2.313	1.43	2.24	2.30	-2.00	82.4	17.6	20.0:79.4	82.2	17.8	15.8:84.2	8
5	2.268(10)	2.267	1.54	1.25	2.53	-1.85	74.2	25.8	10.3:89.4	74.3	25.7	9.8:90.0	8
6	2.183(3)	2.223	1.50	–	3.64	-2.01	68.0	32.0	5.2:94.4	75.8	24.2	8.1:91.8	this work

^aAll molecules geometry optimized without symmetry constraints at the BP TZP/ZORA level. ^bExpl $U-C$ distance (\AA). ^cCalcd $U-C$ distance (\AA). ^dNalewajski–Mrozek bond indices. ^eMDC-m α -spin density on uranium. ^fMDC-q charge on uranium. ^gMDC-q charge on carbene. ^hNatural Bond Orbital (NBO) analysis.

and a very recent report of divergent oxidation chemistry of *N*-oxides toward $[\text{UN}^n]_3$ [$N^n = \text{N}(\text{SiMe}_3)_2$].²⁹

Discussion of a Density Functional Theoretical Analysis of $\text{U}^{\text{IV}}=\text{C}$, $\text{U}^{\text{V}}=\text{C}$, and $\text{U}^{\text{VI}}=\text{C}$ Double Bonds.

Complex **6** is a rare example of a uranium mono-oxo complex^{28b,29,30} the first example of a hexavalent uranium-carbene, and in common with **4** and **5** it possesses a meridionally coordinated chelating BIPM carbene ligand and two axial halides. Thus, given the very close structural relationship of **6** to **4** and **5** these results present the first opportunity to compare the nature and changes in composition of $\text{U}=\text{C}$ double bonds as a function of three oxidation states $\text{U}(\text{IV}-\text{VI})$. We therefore carried out restricted DFT calculations on the full structure of **6**. A comparison of the calculated data to those for **4**, **5**, and **6** is listed in Table 1. Calculated bond lengths and angles for **4-6** are within 0.05 Å and 2°, so we conclude the models provide qualitative descriptions of the bonding in **4-6**. The calculations show significant charge donation from the carbene ligands to uranium in **4-6** and the calculated carbene charges are consistent with formally dianionic centers. Visualization of the frontier orbitals of **6** (Figure 4) shows the σ - and π -components of the $\text{U}=\text{C}$

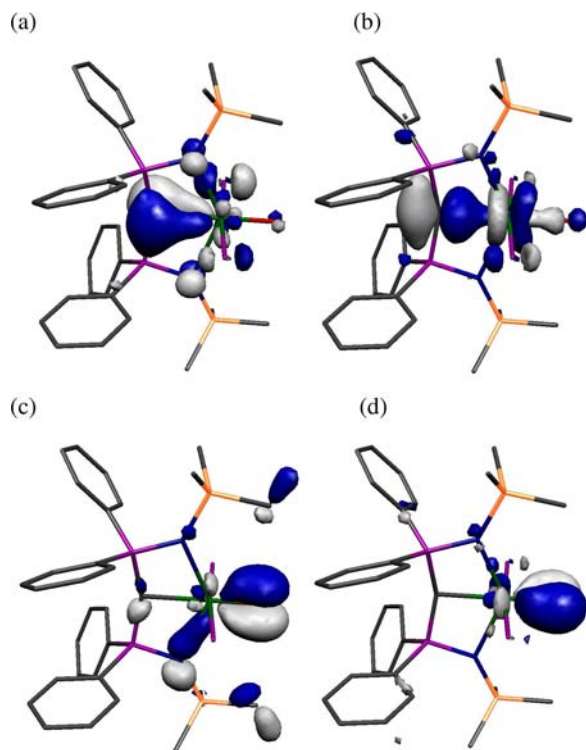


Figure 4. Selected α -spin Kohn–Sham frontier molecular orbitals of **6**, hydrogen atoms omitted for clarity: (a) HOMO (215a, -5.440 eV); (b) HOMO–1 (214a, -5.868 eV); (c) HOMO–24 (191a, -8.198 eV); (d) HOMO–26 (189a, -8.312 eV).

double bond, and the Nalewajski–Mrozek bond indices show significant multiple bond character. For **6** the uranium-oxo calculated bond index is 2.71, which suggests a formal uranium-oxo triple bond. Whereas both the σ - and π -components of the $\text{U}=\text{C}$ double bond are well defined, only the π -components of the uranium–oxygen bond are clear-cut. Several molecular orbitals contribute to the σ -component of the uranium–oxygen bond. Therefore, ITI contributions cannot be delineated.^{30j} However, it should be noted that the HOMO–1

molecular orbital of **6** exhibits a modest σ -component in the uranium–oxo bond as well as the dominant σ -component to the $\text{U}=\text{C}$ double bond which is suggestive of some uranyl-type character (see below).²⁷

We performed NBO analyses to obtain a localized and more chemically relevant description of the $\text{U}=\text{C}$ double bonds in **4-6**. These analyses show polarized $\text{U}=\text{C}$ double bonds in each case. Upon oxidation from uranium(IV) to (V) to (VI) the uranium contribution to the σ -component nearly doubles overall; within the uranium component of the σ -bond the 6d contribution falls from 20 to 10 to 5% with a concomitant increase in 5f orbital contribution. For the π -component, the uranium contribution reaches a maximum at uranium(V) and then falls slightly on oxidation to uranium(VI). However, within the uranium contribution to the π -component the 5f and 6d contributions continue to increase and decrease, respectively, although the magnitude of the change is smaller for the oxidation from uranium(V) to uranium(VI) than for the oxidation from uranium(IV) to uranium(V). Thus, it appears that the oxidation state at uranium has a significant effect on the nature of the $\text{U}=\text{C}$ double bond in **4-6**. In particular, **6** has a lower bond index and a more polarized π -bond than **5**. Increasing the oxidation state of uranium increases its polarizing power but this must compete against an inevitable radial contraction of valence orbitals; based on the NBO data we suggest that the latter may be starting to outweigh the former in **6** compared to **5**.

It is instructive to compare the bonding in **6** to those complexes containing $[\text{E}=\text{U}=\text{O}]^{2+}$ ($\text{E} = \text{O}, \text{N}, \text{C}$) units. Computational studies reveal $\sigma^2\pi^4$ bonding with each molecular orbital delocalized equally over the three-atom units of OUO ,³¹ NUN ,³² and CUC .^{20d} due to their symmetrical environments. However, in EUO species where $\text{E} \neq \text{O}$ the symmetry is broken and bonding orbitals become more localized and clearly defined as deriving from UE or UO bonds.^{20a,28a} This deconvolution is also evident in **6** which reflects the different electronegativities of oxygen and carbon. Thus, although **6** can be regarded as a uranyl analogue, distinct, intrinsic differences in the bonding manifold compared to uranyl are evident.

Topological Analyses of $\text{U}^{\text{IV}}=\text{C}$, $\text{U}^{\text{V}}=\text{C}$, and $\text{U}^{\text{VI}}=\text{C}$ Double Bonds.

In order to examine the nature of the $\text{U}=\text{C}$ bonds in **4-6** we performed topological analyses of the electron densities using Bader's Atoms in Molecules (QTAIM).³³ To place these results in context in order to allow meaningful comparisons, we also carried out QTAIM analyses on the geometry optimized structures of structurally related and authenticated methanide and carbene complexes $[(\text{BIPMH})\text{UCl}_3(\text{THF})]$ (**7**),^{6f} $[(\text{BIPMH})\text{Yl}_2(\text{THF})]$ (**8**),^{13a} $[(\text{BIPM})\text{Yl}(\text{THF})_2]$ (**9**),³⁴ $[(\text{BIPM})\text{Y}(\text{CH}_2\text{SiMe}_3)(\text{THF})]$ (**10**),³⁵ and $[(\text{BIPM})\text{Y}(\text{CH}_2\text{Ph})(\text{THF})]$ (**11**).³⁶ The results of the QTAIM analyses are shown in Table 2. For a covalent bond the electron density $[\rho(\mathbf{r})]$ at the bond critical point (BCP) is usually >0.2 , and for ionic bonds this value is <0.1 . Thus, the $\text{U}=\text{C}$ double bonds in **4-6** appear to possess some covalent character. This view is reinforced through comparison with the uranium-methanide **7**, which possesses a smaller value of $\rho(\mathbf{r})$. Furthermore, the $\rho(\mathbf{r})$ for the yttrium-methanide **8**, which would be predicted to be predominantly ionic, is even smaller, and the ionic yttrium-carbenes **9-11** exhibit $\rho(\mathbf{r})$ values that are only marginally larger than those of **7** and **8**, yet significantly smaller than those of **4-6**. For covalent bonds the Laplacian of the electron density $[\nabla^2\rho(\mathbf{r})]$ is usually negative, indicating a concentration of electron density in the

Table 2. Calculated QTAIM U=C, U–C, Y–C, and Y=C Bond Critical Point Data for 4–11

entry ^a	$w\rho(r)$	$\nabla^2\rho(r)$	$G(r)$	$V(r)$	$H(r)$
4	0.1037	0.1203	0.0697	−0.1093	−0.0396
5	0.1167	0.1017	0.0752	−0.1249	−0.0497
6	0.1302	0.0529	0.0741	−0.1350	−0.0609
7	0.0415	0.0828	0.0263	−0.0319	−0.0056
8	0.0371	0.0818	0.0236	−0.0267	−0.0031
9	0.0638	0.1348	0.0467	−0.0598	−0.0130
10	0.0603	0.1295	0.0431	−0.0539	−0.0108
11	0.0650	0.1311	0.0460	−0.0592	−0.0132

^aAll molecules geometry optimized without symmetry constraints at the BP TZP/ZORA level.

internuclear region. However, the $\nabla^2\rho(r)$ term derives from three curvature values ($\lambda_1, \lambda_2, \lambda_3$) where λ_1 and λ_2 are negative but λ_3 is positive. For first-row elements the overall term is usually negative, but for second-row and heavier elements the λ_3 term often dominates the Laplacian which results in a positive term overall,³⁷ as observed for 4–11. The electronic energy density $H(r)$ of the charge distribution is defined as $H(r) = G(r) + V(r)$, where $G(r)$ is the kinetic energy density and $V(r)$ is the potential energy. For a covalent bond $H(r)$ is usually negative. With the above considerations noted, it is significant that 6 exhibits the largest $\rho(r)$, smallest $\nabla^2\rho(r)$, and most negative $H(r)$ terms, followed by 5 and then 4. This suggests that the covalency within the U=C double bonds of 4–6 decreases in the order 6 > 5 > 4 as supported qualitatively by the DFT and NBO analyses described above (Table 1).

Preliminary Reactivity Study of a Uranium(VI)-Carbene. A preliminary reactivity study of 6 revealed metallo-Wittig reactivity toward 9-anthracene carboxaldehyde and benzaldehyde to give the anticipated colorless alkenes ($\text{Me}_3\text{SiNPPPh}_2$)₂C=C(H)R [R = 9-anthracene (12)⁸ or phenyl (13)], in 41 and 65%, respectively, with concomitant elimination of uranyl dichloride,³⁸ Scheme 1. This parallels the reactivity of uranium(IV/V)-carbenes, further supporting the formulation of 6, but contrasts to the reactivity of yttrium analogues which engage in C–H activation chemistry.³⁹ We suggest this difference in reactivity may derive from the greater covalency of U=C bonds compared to formal Y=C bonds which results in mild [2+2]-cycloaddition and σ -bond metathesis for the former compared to more aggressive C–H activation reactions for the latter.

CONCLUSIONS

To conclude, attempts to prepare a uranyl(VI)-carbene by a deprotonation strategy have resulted in reduction and isolation of the first examples of organometallic uranyl(V) complexes which exhibit rare uranyl(VI)-uranyl(V) cation–cation interactions. Oxidation of a uranium(IV)-carbene with 4-morpholine *N*-oxide afforded the first uranium(VI)-carbene, which contains a [R₂C=U=O]²⁺ analogue of the uranyl ion, and this has permitted a comparison of the nature of U=C double bonds over three oxidation states (IV–VI) for the first time.

EXPERIMENTAL SECTION

Preparation of [UO₂(BIPMH)(μ -Cl)UO(μ -O)(BIPMH)] (2). THF (20 mL) was added to a precooled (−78 °C) mixture of 1 (1.87 g, 2 mmol) and NaCH₂Ph (0.15 g, 1.33 mmol). The reaction mixture was allowed to warm to room temperature and was stirred for 16 h to give a red-brown suspension. Volatiles were removed in vacuo and the

residue was recrystallized from toluene (2 mL) to afford 2 as yellow crystals. Yield: 1.36 g, 80%. Anal. Calcd for C₆₂H₇₈ClN₄O₄P₄Si₄U₂: C, 44.03; H, 4.65; N, 3.31. Found: C, 44.08; H, 4.54; N, 3.06. $\mu_{\text{eff}} = 2.59 \mu_{\text{B}}$ (Evans's method). ¹H NMR (d₆-benzene, 298 K): δ −9.68 (br, 18H, U(V) Si(CH₃)₃), −4.14 (br, 1H, U(V) HCP₂), 0.38 (s, 18H, U(VI) Si(CH₃)₃), 2.24 (br, 4H, U(V) p-Ar-H), 3.40 (t, 1H, ²J_{PH} = 14 Hz, U(VI) HCP₂), 7.12 (m, 8H, U(VI) Ar-H), 7.43 (m, 8H, U(VI) Ar-H), 7.80 (m, 4H, U(VI) p-Ar-H), 8.15 (br, 8H, U(V) m-Ar-H), 12.09 (br, 4H, U(V) o-Ar-H) and 14.52 (br, 4H, U(V) o-Ar-H). ³¹P{¹H} NMR (d₆-benzene, 298 K): δ −5.16, −129.42 (br). FTIR ν/cm^{-1} (Nujol): 1589 (w), 1260 (m), 1243 (m), 1110 (s), 1092 (s), 1028 (m), 906 (m), 834 (s), 803 (m), 721 (m), 692 (m). The formation of dibenzyl was confirmed by NMR spectroscopy and GC-MS. A fraction that eluted at 11.2 min gave *m/z* peaks at 91.04 and 182.05 which correspond to PhCH₂ and PhCH₂CH₂Ph. This was compared to an authentic sample of PhCH₂CH₂Ph which gave an exact match for retention time, fragmentation pattern and peak masses, confirming the formation of PhCH₂CH₂Ph.

Preparation of [UO(μ -O)(BIPMH)(μ -Cl){UO(μ -O)(BIPMH)}₂] (3). From the reaction which yielded 2 we also isolated a small number of red crystals of 3 by fractional crystallization. Yield: 0.02 g, 2%. Anal. Calcd for C₉₃H₁₁₇ClN₆O₆P₆Si₆U₃: C, 44.34; H, 4.68; N, 3.34. Found: C, 43.79; H, 4.33; N, 3.17. $\mu_{\text{eff}} = 4.01 \mu_{\text{B}}$ (Evan's method). ¹H NMR (d₆-benzene, 298 K): δ −6.18 (br, 18H, U(V) Si(CH₃)₃), −4.27 (br, 2H, U(V) HCP₂), 0.27 (s, 18H, U(VI) Si(CH₃)₃), 1.33 (s, 2H, U(V) Ar-H), 2.65 (d, 4H, ³J_{HH} = 6 Hz, U(V) Ar-H), 3.28 (t, 1H, ²J_{PH} = 13.6 Hz, U(VI) HCP₂), 4.58 (br, 18H, U(VI) Si(CH₃)₃ and 4H, U(V) Ar-H), 5.26 (t, 4H, ³J_{HH} = 6 Hz, U(V) Ar-H), 5.71 (t, 4H, ³J_{HH} = 6 Hz, U(V) Ar-H), 7.02 (m, 12H, U(VI) Ar-H), 7.68 (m, 8H, U(VI) o-Ar-H), 8.41 (t, 2H, ³J_{HH} = 6 Hz, U(V) Ar-H), 8.45 (t, 2H, ³J_{HH} = 6 Hz, U(V) Ar-H), 8.70 (t, 2H, ³J_{HH} = 6 Hz, U(V) Ar-H), 8.88 (d, 4H, ³J_{HH} = 6 Hz, U(V) Ar-H), 8.93 (s, 2H, U(V) Ar-H), 9.77 (s, 4H, U(V) Ar-H), 10.09 (br s, 2H, U(V) Ar-H), 11.17 (s, 4H, U(V) Ar-H). ³¹P{¹H} NMR (d₆-benzene, 298 K): δ 5.17, −139.13 (br), −159.74 (br). FTIR ν/cm^{-1} (Nujol): 1589 (w), 1261 (m), 1091 (br, s), 1020 (m), 900–802 (br, m), 723 (m).

Preparation of [(BIPM)UOCl₂] (6). Toluene (10 mL) was added to a precooled (−78 °C) mixture of 4 (1.09 g, 1.00 mmol) and 4-morpholine *N*-oxide (0.13 g, 1.10 mmol). The mixture was then allowed to slowly warm to room temperature with stirring over 18 h to afford a dark brown solution. The solution was filtered, reduced in volume (~3 mL), and then stored at −30 °C to afford 6 as brown crystals. Yield: 0.46 g, 52%. Anal. Calcd for C₃₁H₃₈Cl₂IN₂P₂Si₂U: C, 45.79; H, 4.66; N, 2.95. Found: C, 45.70; H, 4.65; N, 2.93. ¹H NMR (d₆-benzene, 298 K): δ 0.61 (s, 18H, Si(CH₃)₃), 7.12–7.28 (br m, 12H, *m/p*-CH(Ar)), 7.71 (m, 8H, *o*-CH(Ar)). ¹³C{¹H} NMR (d₆-benzene, 298 K): δ 1.36 (Si(CH₃)₃), 129.11 (Ar-C), 131.88 (Ar-C), 132.71 (Ar-C), 139.05 (Ar-C). The carbene resonance for 6 was not observed in the ¹³C{¹H} NMR spectrum recorded in d₆-benzene due to the poor solubility of 6 in arene solvents once recrystallized; however, the NMR spectra are clearly diamagnetic which is consistent with the uranium(VI) formulation of 6. Complex 6 is unstable in polar solvents such as THF and pyridine and decomposes to H₂C-(PPh₂NSiMe₃)₂ and unidentified uranium-containing products which precluded recording of NMR spectra in these solvents. ²⁹Si{¹H} NMR (d₆-benzene, 298 K): δ −0.69. ³¹P{¹H} NMR (d₆-benzene, 298 K): δ −29.1. FTIR ν/cm^{-1} (Nujol): 1589 (w), 1437 (s), 1211 (s), 1114 (vs), 1044 (br), 917 (s, U=O), 845 (s).

Preparation of (Me₃SiNPPPh₂)₂C=C(H)R (12, R = 9-anthracene). 9-anthracenecarboxaldehyde (0.11 g, 0.55 mmol) in toluene (10 mL) was added dropwise to a precooled (−78 °C) suspension of 6 (0.44 g, 0.50 mmol) in toluene (10 mL). The dark red reaction mixture was allowed to warm to room temperature and was stirred for 66 h to give a gray reaction mixture. The solution was filtered from the resulting precipitate and volatiles were removed in vacuo to afford a gray solid. The gray solid was recrystallized from acetonitrile (5 mL) to give colorless crystals of 12. Yield: 0.15 g, 41%. Analysis of the crude mixture by multinuclear NMR showed quantitative conversion. The precipitate was recrystallized from THF to afford a yellow crystalline material which was identified as [(UO₂Cl₂(THF)₂)₂] by comparison

to an authentic sample.³⁸ Compound **12** was authenticated by comparison to an authentic sample.⁸

Preparation of (Me₃SiNPPPh₂)₂C=C(H)R (13**, R = Ph).** Benzaldehyde (0.059 g, 0.55 mmol) in toluene (10 mL) was added dropwise to a precooled (−78 °C) suspension of **6** (0.44 g, 0.50 mmol) in toluene (10 mL). The dark yellow reaction mixture was allowed to warm to room temperature and stirred for 66 h to give a gray reaction mixture. The solution was filtered from the resulting precipitate and volatiles were removed in vacuo to afford a gray solid. The gray solid was recrystallized from acetonitrile (5 mL) to give colorless crystals of **13**. Yield: 0.21 g, 65%. Analysis of the crude mixture by multinuclear NMR showed quantitative conversion. The precipitate was recrystallized from THF to afford a yellow crystalline material which was identified as [UO₂Cl₂(THF)₂]₂ by comparison to an authentic sample.³⁸ Anal. Calcd for C₃₈H₄₄P₂N₂Si₂: C, 70.55; H, 6.85; N, 4.33. Found: C, 70.71; H, 6.75; N, 4.23. ¹H NMR (d₆-benzene, 298 K): δ 0.49 (s, 9 H, NSi(CH₃)₃), 0.50 (s, 9 H, NSi(CH₃)₃), 6.91 (br, 2H, m-Ph-CH), 7.01 (br, 8H, m-Ph-CH P), 7.28 (br, 6H, p-Ph-CH P and o-Ph-CH), 7.51 (br, 1H, p-Ph-CH), 7.88 (m, 8H, o-Ph-CH), 8.15 (dd, ³J_{PH} = 36.2 and 48.4 Hz, 1H, PhHC=CP₂). ¹³C{¹H} NMR (d₆-benzene, 298 K): δ 4.13 (d, J_{PC} = 3.0 Hz, Si(CH₃)₃), 4.34 (d, J_{PC} = 3.0 Hz, Si(CH₃)₃), 127.29 (d, J_{PC} = 3.7 Hz, m-Ph-CH P), 127.98 (d, J_{PC} = 3.7 Hz, m-Ph-CH P), 128.97 (m-Ph-CH), 129.92 (p-Ph-CH), 130.46 (o-Ph-CH), 130.75 (p-Ph-CH P), 132.06 (d, ²J_{PC} = 10.6 Hz, o-Ph-CH P), 132.40 (d, ²J_{PC} = 10.6 Hz, o-Ph-CH P), 134.44 (d, J_{PC} = 66.4 Hz ipso-Ph-C P), 135.83 (s, ipso-Ph-C), 135.97 (dd, J_{PC} = 41.3 and 98.6 Hz, PhHC=CP₂), 157.61 (d, ²J_{PC} = 7.1 Hz, PhHC=CP₂). ³¹P{¹H} NMR (d₆-benzene, 298 K): δ −7.64 (d, ²J_{PP} = 34.8 Hz), −6.87 (d, ²J_{PP} = 34.8 Hz). ²⁹Si{¹H} NMR (d₆-benzene, 298 K): δ −12.51 (d, ²J_{PSi} = 39.8 Hz), −12.02 (d, ²J_{PSi} = 39.8 Hz). FTIR ν/cm^{−1} (Nujol): 1553 (m, C=C), 1314 (s), 1299 (s), 1234 (m), 823 (s), 748 (m), 695 (m), 681 (m).

■ ASSOCIATED CONTENT

● Supporting Information

General experimental considerations and spectroscopic, magnetometric, electrochemical, crystallographic, and computational details for **2**, **3**, **6–13** (CIF, PDF). This material is available free of charge via the Internet at <http://pubs.acs.org>.

■ AUTHOR INFORMATION

Corresponding Author

stephen.liddle@nottingham.ac.uk

Notes

The authors declare no competing financial interest.

■ ACKNOWLEDGMENTS

We thank the Royal Society, the EPSRC, the ERC, the University of Nottingham, COST Action CM1006, and the National Nuclear Laboratory for generous support of this work.

■ REFERENCES

- (1) Nugent, W. A.; Mayer, J. M. *Metal-Ligand Multiple Bonds*; John Wiley & Sons: New York, 1988.
- (2) (a) Sierra, M. A. *Chem. Rev.* **2000**, *100*, 3591. (b) Schrock, R. R. *Chem. Rev.* **2002**, *102*, 145. (c) Scott, J.; Mendiola, D. J. *Dalton Trans.* **2009**, 8463.
- (3) (a) Giesbrecht, G. R.; Gordon, J. C. *Dalton Trans.* **2004**, 2387. (b) Hayton, T. W. *Dalton Trans.* **2010**, 39, 1145.
- (4) (a) Cramer, R. E.; Maynard, R. B.; Paw, J. C.; Gilje, J. W. *J. Am. Chem. Soc.* **1981**, *103*, 3598. (b) Gilje, J. W.; Cramer, R. E. *Inorg. Chim. Acta* **1987**, *139*, 177 and references therein. (c) Cramer, R. E.; Bruck, M. A.; Edelmann, F.; Afzal, D.; Gilje, J. W.; Schmidbaur, H. *Chem. Ber.* **1988**, *121*, 417.
- (5) During this time uranium carbenes were implicated in McMurray-type reactions, observed in matrix isolation experiments, and computationally examined. See: (a) Villiers, C.; Ephritikhine, M.

Chem.—Eur. J. **2001**, *7*, 3043. (b) Lyon, J. T.; Andrews, L.; Hu, H.-S.; Li, J. *Inorg. Chem.* **2008**, *47*, 1435. (c) Yahia, A.; Castro, L.; Maron, L. *Chem.—Eur. J.* **2010**, *16*, 5564.

(6) (a) Cantat, T.; Arliguie, T.; Noël, A.; Thuéry, P.; Ephritikhine, M.; Le Floch, P.; Mézailles, N. *J. Am. Chem. Soc.* **2009**, *131*, 963. (b) Tourneux, J.-C.; Berthet, J.-C.; Thuéry, P.; Mézailles, N.; Le Floch, P.; Ephritikhine, M. *Dalton Trans.* **2010**, 39, 2494. (c) Cooper, O. J.; McMaster, J.; Lewis, W.; Blake, A. J.; Liddle, S. T. *Dalton Trans.* **2010**, 39, 5074. (d) Fortier, S.; Walensky, J. R.; Wu, G.; Hayton, T. W. *J. Am. Chem. Soc.* **2011**, *133*, 6894. (e) Tourneux, J.-C.; Berthet, J.-C.; Cantat, T.; Thuéry, P.; Mézailles, N.; Le Floch, P.; Ephritikhine, M. *Organometallics* **2011**, *30*, 2957. (f) Mills, D. P.; Moro, F.; McMaster, J.; van Slageren, J.; Lewis, W.; Blake, A. J.; Liddle, S. T. *Nature Chem.* **2011**, *3*, 454. (g) Ma, G.; Ferguson, M. J.; McDonald, R.; Cavell, R. G. *Inorg. Chem.* **2011**, *50*, 6500.

(7) Tourneux, J.-C.; Berthet, J.-C.; Cantat, T.; Thuéry, P.; Mézailles, N.; Ephritikhine, M. *J. Am. Chem. Soc.* **2011**, *133*, 6162.

(8) Cooper, O. J.; Mills, D. P.; McMaster, J.; Moro, F.; Davies, E. S.; Lewis, W.; Blake, A. J.; Liddle, S. T. *Angew. Chem., Int. Ed.* **2011**, *50*, 2383.

(9) We make a clear distinction between uranyl, which forms a class in its own right, and other hexavalent uranium complexes. See ref 12.

(10) (a) Hallwachs, H.; Schafarick, A. *Ann. Chem.* **1859**, *109*, 206. (b) Sand, J.; Singer, F. *Justus Liebigs Ann. Chem.* **1903**, *329*, 190.

(11) (a) Sarsfield, M. J.; Helliwell, M.; Collison, D. *Chem. Commun.* **2002**, 2264. (b) Sarsfield, M. J.; Steele, H.; Helliwell, M.; Teat, S. J. *Dalton Trans.* **2003**, 3443. (c) Maynadié, J.; Berthet, J.-C.; Thuéry, P.; Ephritikhine, M. *Chem. Commun.* **2007**, 486.

(12) Ephritikhine, M. *Dalton Trans.* **2006**, 2501.

(13) (a) Liddle, S. T.; Mills, D. P.; Gardner, B. M.; McMaster, J.; Jones, C.; Woodul, W. D. *Inorg. Chem.* **2009**, *48*, 3520. (b) Wooles, A. J.; Cooper, O. J.; McMaster, J.; Lewis, W.; Blake, A. J.; Liddle, S. T. *Organometallics* **2010**, *29*, 2315.

(14) For comprehensive reviews and references therein see: (a) Graves, C. R.; Kiplinger, J. L. *Chem. Commun.* **2009**, 3831. (b) Hayton, T. W. *Dalton Trans.* **2010**, 39, 1145. (c) Fortier, S.; Hayton, T. W. *Coord. Chem. Rev.* **2010**, *254*, 197. (d) Arnold, P. L.; Love, J. B.; Patel, D. *Coord. Chem. Rev.* **2010**, *254*, 19753.

(15) Edelstein, N. M.; Lander, G. H. *The Chemistry of the Actinide and Transactinide Elements*; Springer: Dordrecht, 2006.

(16) Sullivan, J. C.; Zielen, A. J.; Hindman, J. C. *J. Am. Chem. Soc.* **1961**, *83*, 3373.

(17) Mougél, V.; Horeglad, P.; Nocton, G.; Pécaut, J.; Mazzanti, M. *Angew. Chem., Int. Ed.* **2009**, *48*, 8477.

(18) (a) Sarsfield, M. J.; Helliwell, M. *J. Am. Chem. Soc.* **2004**, *126*, 1036. (b) Sullens, T. A.; Jensen, R. A.; Shvareva, T. Y.; Albrecht-Schmitt, T. E. *J. Am. Chem. Soc.* **2004**, *126*, 2676. (c) Burns, P. C.; Kubatko, K.-K. *Inorg. Chem.* **2006**, *45*, 10277.

(19) (a) Lovely, D. R.; Phillips, E. J. P.; Gorby, Y. A.; Landa, E. R. *Nature* **1991**, *350*, 413. (b) Renshaw, J. C.; Butchins, L. J. C.; Livens, F. R.; May, I.; Charnock, J. M.; Lloyd, J. R. *Environ. Sci. Technol.* **2005**, *39*, 5657. (c) Ilton, E. S.; Haiduc, A.; Cahill, C. L.; Felmy, A. R. *Inorg. Chem.* **2005**, *44*, 2986.

(20) CUO has been observed in matrix isolation experiments, see: (a) Zhou, M.; Andrews, L.; Li, J.; Bursten, B. E. *J. Am. Chem. Soc.* **1999**, *121*, 9712. (b) Li, J.; Bursten, B. E.; Liang, B.; Andrews, L. *Science* **2002**, *295*, 2242. (c) Andrews, L.; Liang, B.; Li, J.; Bursten, B. E. *J. Am. Chem. Soc.* **2003**, *125*, 3126. (d) Wang, X.; Andrews, L.; Malmqvist, P.; Roos, B. O.; Gonçalves, A. P.; Pereira, C. C. L.; Marçalo, J.; Godart, C.; Villeroy, B. *J. Am. Chem. Soc.* **2010**, *132*, 8484.

(21) For example, treatment of a bis(imido) uranyl analogue resulted in reduction. See: Spencer, L. P.; Schelter, E. J.; Yang, P.; Gdula, R. L.; Scott, B. L.; Thompson, J. D.; Kiplinger, J. L.; Batista, E. R.; Boncella, J. M. *Angew. Chem., Int. Ed.* **2009**, *48*, 3795.

(22) Magnetic moments for UO₂⁺ complexes that exceed the theoretical moment for ²F_{5/2} have been reported. For example, see: (a) Nocton, G.; Horeglad, P.; Pécaut, J.; Mazzanti, M. *J. Am. Chem. Soc.* **2008**, *130*, 16633. (b) Nocton, G.; Horeglad, P.; Vetere, V.;

Pécaut, J.; Dubois, L.; Maldivi, P.; Edelstein, N. M.; Mazzanti, M. *J. Am. Chem. Soc.* **2010**, *132*, 495.

(23) See the Supporting Information for full details.

(24) (a) Berthet, J.-C.; Siffredi, G.; Thuéry, P. T.; Ephritikhine, M. *Chem. Commun.* **2006**, 3184. (b) Natrajan, L.; Burdet, F.; Pécaut, J.; Mazzanti, M. *J. Am. Chem. Soc.* **2006**, *128*, 7152. (c) Hayton, T. W.; Wu, G. *J. Am. Chem. Soc.* **2008**, *130*, 2005.

(25) As evidenced from a search of the Cambridge Structural Database (CSD version 1.11, date: 25/04/2012): (a) Allen, F. H. *Acta Crystallogr. Sect. B* **2002**, *58*, 380.

(26) "Missing" shadow components in solid-state structures with disordered uranium complexes are known: Evans, W. J.; Walensky, J. R.; Ziller, J. W. *Organometallics* **2010**, *29*, 945.

(27) Kaltsoyannis, N. *Chem. Soc. Rev.* **2003**, *32*, 9.

(28) (a) Hayton, T. W.; Boncella, J. M.; Scott, B. L.; Batista, E. R. *J. Am. Chem. Soc.* **2006**, *128*, 12622. (b) Fortier, S.; Wu, G.; Hayton, T. W. *J. Am. Chem. Soc.* **2010**, *132*, 6888.

(29) Fortier, S.; Brown, J. L.; Kaltsoyannis, N.; Wu, G.; Hayton, T. W. *Inorg. Chem.* **2012**, *51*, 1625.

(30) (a) Arney, D. S.; Burns, C. J. *J. Am. Chem. Soc.* **1993**, *115*, 9840. (b) Brown, D. R.; Denning, R. G.; Jones, R. H. *Chem. Commun.* **1994**, 2601. (c) Williams, V. C.; Muller, M.; Leech, M. A.; Denning, R. G.; Green, M. L. H. *Inorg. Chem.* **2000**, *39*, 2538. (d) Roussel, P.; Boaretto, R.; Kingsley, A. J.; Alcock, N. W.; Scott, P. *J. Chem. Soc., Dalton Trans.* **2002**, 1423. (e) Evans, W. J.; Kozimor, S. A.; Ziller, J. W. *Polyhedron* **2004**, *23*, 2689. (f) Zi, G.; Jia, L.; Werkema, E. L.; Walter, M. D.; Gottfriedsen, J. P.; Andersen, R. A. *Organometallics* **2005**, *24*, 4251. (g) Bart, S. C.; Anthon, C.; Heinemann, F. W.; Bill, E.; Edelstein, N. M.; Meyer, K. *J. Am. Chem. Soc.* **2008**, *130*, 12536. (h) Kraft, S. J.; Walensky, J.; Fanwick, P. E.; Hall, M. B.; Bart, S. C. *Inorg. Chem.* **2010**, *49*, 7620. (i) Fortier, S.; Kaltsoyannis, N.; Wu, G.; Hayton, T. W. *J. Am. Chem. Soc.* **2011**, *133*, 14224. (j) Kosog, B.; La Pierre, H. S.; Heinemann, F. W.; Liddle, S. T.; Meyer, K. *J. Am. Chem. Soc.* **2012**, *134*, 5284.

(31) Pepper, M.; Bursten, B. E. *Chem. Rev.* **1991**, *91*, 719.

(32) Hayton, T. W.; Boncella, J. M.; Scott, B. L.; Palmer, P. D.; Batista, E. R.; Hay, P. J. *Science* **2005**, *310*, 1941.

(33) (a) Bader, R. F. W. *Atoms in Molecules: A Quantum Theory*; Oxford University Press: New York, 1990. (b) Bader, R. F. W. *J. Phys. Chem. A* **1998**, *102*, 7314.

(34) Mills, D. P.; Wooles, A. J.; McMaster, J.; Lewis, W.; Blake, A. J.; Liddle, S. T. *Organometallics* **2009**, *28*, 6771.

(35) Liddle, S. T.; McMaster, J.; Green, J. C.; Arnold, P. L. *Chem. Commun.* **2008**, 1747.

(36) Mills, D. P.; Cooper, O. J.; McMaster, J.; Lewis, W.; Liddle, S. T. *Dalton Trans.* **2009**, 4547.

(37) (a) Coppens, P. *X-ray Charge Densities and Chemical Bonding*; IUCr Oxford University Press: New York, 1997. (b) Popelier, P. *Atoms in Molecules An Introduction*; Pearson Education: Harlow, England, 2000.

(38) Wilkerson, M. P.; Burns, C. J.; Paine, R. T.; Scott, B. L. *Inorg. Chem.* **1999**, *38*, 4156.

(39) Mills, D. P.; Soutar, L.; Lewis, W.; Blake, A. J.; Liddle, S. T. *J. Am. Chem. Soc.* **2010**, *132*, 14379.